

UNDERWATER SOUND PROJECTORS

Electroacoustic transducers convert electric signals into acoustic signals, or vice versa. Most transducers, in principle, function as either transmitters or receivers. However they are usually specialized for one task or the other. In the underwater realm transducers that are specialized to emit sound are called projectors, and those specialized as receivers are called hydrophones. This article describes many devices meeting the definition of projector but excludes sound generating mechanisms that do not respond to a drive signal, such as sirens, gongs, or direct mechanical-to-acoustical converters (the cam-driven piston, for example), and the parametric array that relies on the nonlinearity of the medium to form the desired acoustic waveform.

Although some underwater sound projectors use the same driver types found in loudspeakers, several factors dictate the use of specialized, more rugged transduction methods than used in air. One factor is the significant static pressure difference usually experienced on opposite sides of the radiating surface in the underwater environment. In contrast, loudspeakers are nearly always statically balanced. A second factor is that the specific acoustic impedance (ratio of pressure to particle velocity) is 3500 times higher in water than in air, so underwater projectors must work at higher stress levels. Finally, the underwater environment is generally harsher with respect to temperature extremes, corrosion, and obstacle impact. Together these considerations lead to higher static and dynamic stresses underwater, which in turn leads to more rugged construction and drivers having intrinsically high mechanical impedance. Although many of the transducer types described here may be designed for use at ultrasonic frequencies, this article concentrates on the sonar frequency range, roughly 20 Hz to 20 kHz. The low end of this range presents particular challenges to the projector designer because the size of the transducer grows quite dramatically at low frequencies. See Refs. 1 and 2 for details.

The first successful underwater sound projector was a moving coil device designed by R. A. Fessenden and used to detect an iceberg in 1914. The onset of World War I stimulated the

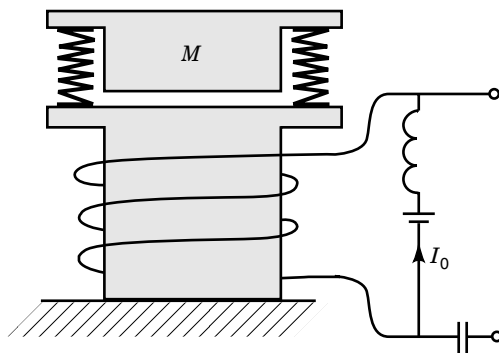


Figure 1. Moving armature (variable reluctance) transduction. The external driving circuit features a blocking coil that prevents the ac driving signal from flowing through the dc bias branch. Similarly, the bias current I_0 is isolated from the signal source by a capacitor.

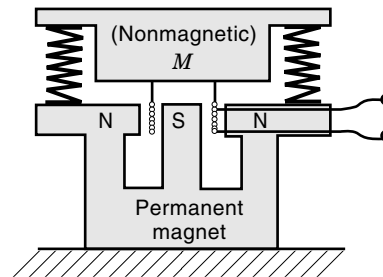


Figure 2. Moving coil (electrodynamic) transduction. Nonlinearities arise when the coil travels beyond the region of uniform radial magnetic field.

development of higher power sound sources to search for submarines, and the first active sonar detection of a submarine was achieved by French physicist Paul Langevin in 1918 at a target range of 8 km, using a quartz mosaic sandwich projector (3).

Types of Excitation (Driver Classification)

Several transduction methods can be considered for underwater projectors. One class of drivers, known as surface-force transducers, converts electricity to useful force at a discontinuity in material properties. Examples of these are the moving armature or variable reluctance type (Fig. 1) in which an electromagnet periodically attracts and releases a sprung radiator plate; the moving coil or electrodynamic type (Fig. 2), the basis of most loudspeakers today; and the electrostatic type (Fig. 3), a capacitor with moving plates. In each case vertical motion of mass M causes sound radiation. For clarity, all supporting structures and waterproofing details have been omitted from Figs. 1 to 5.

The other broad class are body-force transducers in which mechanical distortion is produced in an electrically or magnetically active material. Piezoelectric materials have the property that an electric field applied to the material causes mechanical strain, and, reciprocally, an applied stress produces a voltage. The effect is linear for small and moderate signals. Natural piezoelectric crystals, such as quartz, were used extensively in the early years, but soon piezoelectric ceramics (initially barium titanate, but later mixtures of lead zirconate and lead titanate generally known by their commercial name PZT) were introduced. By the 1960s various PZT formulations became the dominant active materials for underwater projectors. In raw form these materials are termed “electrostrictive” and show a square-law strain/field relation-

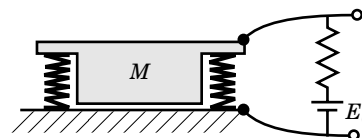


Figure 3. Electrostatic transduction is nonlinear at all amplitudes because electrostatic attraction varies with the square of gap width.

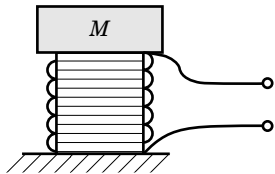


Figure 4. A basic piezoelectric (electrostrictive) driver. Ceramic polarity alternates (up, down, up, down) in adjacent slabs so the electric field excites the same polarity of strain in every slab.

ship, but by applying a polarizing dc field during one stage of manufacture, they become “poled.” Then they show linear strain/field behavior and are called piezoelectric ceramics.

Ceramic transducers are usually designed to have the excitation signal applied in the poled direction. Because ceramic thickness in the poling direction is limited to about 15 mm, placing the polarized axis along a large dimension of the active material requires segmenting it into slabs, inserting electrodes perpendicular to the desired electric field, and connecting the electrodes in parallel. This permits lower voltage levels and provides a better electrical impedance match to the amplifier. Because they are produced in a ceramic firing process, piezoelectric ceramics have some variability in properties and are quite brittle (have little tensile or shear strength). On the other hand, improved process control limits piece-to-piece variation, compressive prestress can protect against tensile stresses, and casting allows making a great variety of shapes. Figure 4 shows the essential features of a simple segmented-stack piezoelectric driver.

Magnetostrictive materials undergo strain upon application of a magnetic field, although the mechanical response is square-law, not linear. To achieve quasi-linearity, magnetostrictive drivers are also polarized, either by permanent magnets, a separate dc winding, or by superimposing a dc voltage on the ac driving signal. Magnetostrictive transducers were largely eclipsed by piezoelectric transducers until the discovery in the early 1970s that some rare earth/iron alloys exhibit giant magnetostrictive strains. Continued refinement of these materials culminated in the alloy “Terfenol D” which is now the material of choice for magnetostrictive drivers. Although its properties are stress-sensitive and it has a somewhat lower coupling coefficient than PZT, the enormous strain amplitudes possible with this material and its low sound speed make it appealing in low-frequency applications. Figure 5 is a simple form of a magnetostrictive driver.

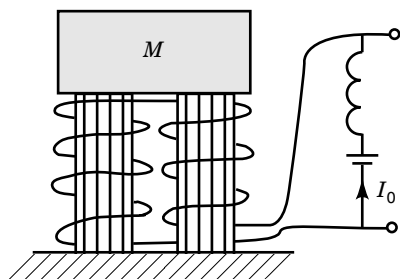


Figure 5. A basic magnetostrictive driver. Both end pieces must have high permeability to complete the magnetic circuit. The function of the blocking coil is described in Fig. 1.

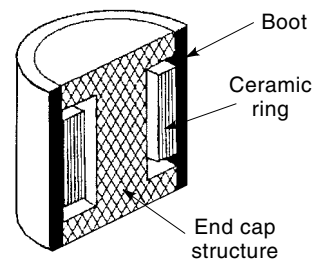


Figure 6. An air-backed cylinder. The ceramic ring may be poled and excited either radially or circumferentially.

The basic driver types depicted in these five figures are examined in more detail following. Reference 4 is recommended as a thorough introduction to transduction theory, and Refs. 5 and 6 provide good introductions to the principles and methods of electroacoustic design.

Practical Transducer Types

This section gives brief nontechnical descriptions of some popular projector types. The sketches emphasize mechanical connections. Wiring schemes are omitted for clarity. Most of these examples are body-force transducers. However, one important surface force type concludes the list. Presenting design methods for every type is beyond the scope of this article. Details will be found in the references.

Air-Backed Cylinder. A thickness-poled, air-backed piezoelectric cylinder (Fig. 6) is suspended between rigid end caps and excited into uniform radial vibration. The surrounding waterproofing sheath is either a sheet rubber boot or a potted encapsulant. The main advantages of this approach are design simplicity, good efficiency, and efficient use of ceramic (because dynamic stresses are uniform throughout the cylinder). A variant, called the *multimode* transducer, has the electric field applied with opposite polarity in different sectors of the cylinder, thus causing circumferential flexure which produces a directive acoustic output pattern (7).

Sphere. A radially-poled ceramic sphere (Fig. 7) makes a simple source having omnidirectional patterns, good bandwidth, and high efficiency. Because hydrostatic pressure produces only compressive shell stresses in a sphere, adequate depth capability is usually obtained. The wire from the electrode on the inner surface is brought out through a small hole in the wall, and the entire assembly is encapsulated. The electroacoustic design of a piezoelectric sphere is straightforward because the radiation impedance of a sphere is known exactly.

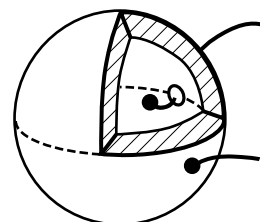


Figure 7. A sphere of radially polarized ceramic. The breathing mode radiates omnidirectionally.

This transducer cannot be hard mounted because the entire outside surface vibrates. It may be suspended by its cable or in a string bag. Small spheres are usually formed from two cast hemispheres bonded at the equator, and larger spheres consist of triangular plates segmented to form polygons.

Longitudinal Vibrator. The most widely-used transducer for high-power shipboard and torpedo sonars is the Tonpizl ("sound mushroom" in German) (Fig. 8). A ceramic cylinder, either a single radially poled piece or a stack of thickness-poled rings, is clamped between two masses by a tie rod. The forward (head) mass flares slightly to form the radiating surface. The rearward (tail) mass is isolated from the acoustic medium. The vibrating assembly is normally encased in a container that provides resilient supports and waterproofing for the wetted face. Placing the tie rod in tension applies a compressive bias stress to the ceramic element. The advantages of this design are efficient utilization of ceramic (dynamic stresses in the drive element are nearly uniform) and the ability to isolate the ceramic stack from hydrostatic pressure. Because of the large number of design parameters, optimizing the design is a challenge. Practical complications include avoiding head flexure, providing for adequate ceramic cooling, and coping with variations in ceramic properties during mass production. Chapters 7 and 8 of Ref. 6, a large part of Ref. 8, and all of Ref. 9 are devoted to longitudinal vibrators.

Flexural Disk. A way to obtain lower operating frequencies for a given size transducer is to shift from longitudinal to flexural modes of motion. Bonding two thickness-poled ceramic disks back to back and wiring them so that one expands radially as the other contracts results in flexure of the bilaminar pair. Because ceramic near the neutral plane is underutilized, a trilaminar configuration, as shown in Fig. 9, is more typical. The inert central plate extends beyond the radius of the two active plates and attaches to an annular hinge which must be radially compliant but axially stiff. Because radial ceramic strains are converted to flexure in the composite disk, high-shear-strength bonds between the three plates are essential. Various means are used to apply circumferential prestress to the ceramic disks. Report (10) is the standard reference work for flexural disk transducers.

Most practitioners use flexural disks in back-to-back configurations with a small air-filled cavity between the disks.

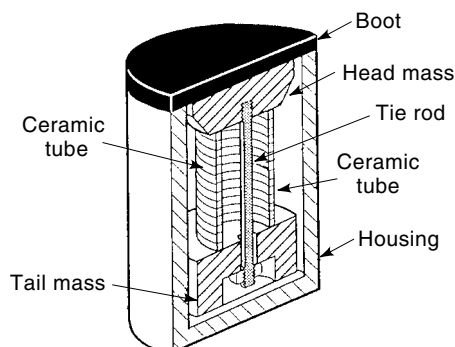


Figure 8. The longitudinal vibrator (Tonpizl), a projector type used in many high-power sonar systems.

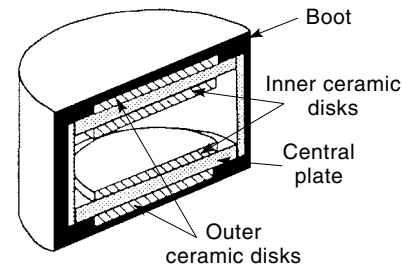


Figure 9. Opposing pairs of flexural disks are usually wired to produce an acoustic monopole (i.e., both outer disks flex outward in phase).

This provides dynamic balancing of the hinge reaction forces and results in a compact low-frequency source. Hydrostatic pressure places the inner ceramic plate in tension, however, thus limiting its depth capability. One solution is to omit the inner ceramic plate. This shifts the neutral plane to be near the bond line, and only the metal central plate experiences tension. The price of this fix is lower sensitivity. Another approach is to place a single trilaminar disk over the mouth of a long flooded pipe that has its far end capped. This *organ pipe* source has unlimited depth capability but very small bandwidth, a combination of qualities which matches the requirements for certain sonic beacons and tomography sources.

Flexural Bar. Changing the geometry of the previous vibrator from circular to rectangular produces the flexural (or "bender") bar (Fig. 10) (11). These are normally arranged like barrel staves around a relatively compliant oil-filled cavity capped by rigid end pieces. The purpose of the central cavity is to absorb the out-of-phase pressure generated by the inner surface of the bars, and the compliance of this cavity is increased by filling it with flattened air-filled metal tubes. Very low frequency designs sometimes have the cavities filled with pressurized gas. Bender bar projectors are often chosen for high-power, low-frequency, moderate depth applications.

Flextensional. Placing the frequency-controlling member in flexure does produce a lower resonance in a given size. Operating the driving element in an extensional mode while only the radiating surface is in flexure yields even lower frequencies and greater relative bandwidth, depending on the materials used. The term *flextensional* alone generally refers to the

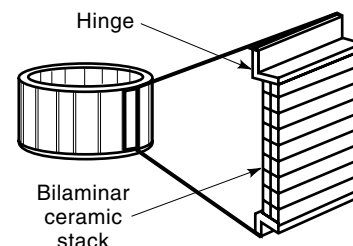


Figure 10. A cylinder of flexural bars. Individual ceramic stacks may be bilaminar (as shown) or trilaminar with an inert central sheet.

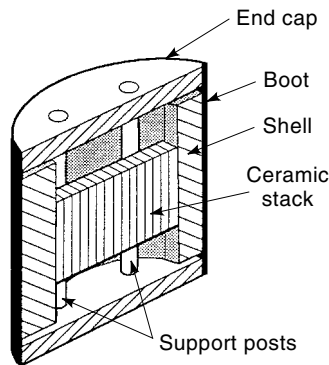


Figure 11. The Class IV flextensional transducer. A single shell/stack assembly is shown, but often these are built with several identical shell/stack assemblies stacked axially and covered by a continuous boot.

configuration depicted in Fig. 11, a driver stack of ceramic or magnetostrictive material placed inside the major axis of an elliptical cylinder. Several other geometries tried result in families of flextensionals, football-shaped, dog-bone shaped, a ring between two concave or convex plates, and other variants on these ideas. But the Fig. 11 shape, known as the Class IV flextensional, has proven most popular. Chapter 13 in Ref. 12 discusses the nomenclature for the different classes, and Ref. 13 reviews the history of this transducer type.

Like bender bars, flextensionals are reliable and provide high source levels at low frequencies from small packages, but in addition they usually provide more bandwidth than benders. Their bandwidth advantage results because the flexing, higher velocity component is made of a lower density material than the electrically active driving component. The ceramic is usually prestressed by statically deforming the surrounding shell rather than by tie rods parallel to the stack(s). Analytical descriptions of the Class IV flextensional are available (14), but most designers now rely on finite-element analysis when designing these complex projectors. One drawback of the classical flextensional is that, at the main resonance, radiation from the sharp ends of the shell near the major axis is out of phase with that from the sides near the minor axis. This can be remedied by making the primary radiating surface concave rather than convex, in which case it is known as a barrel stave flextensional (see Ref. 12 Chaps. 13, 14, and 15).

Ring Shell. One flextensional variant is called the ring-shell projector, (Fig. 12) (15,16). In this design the radiating sur-

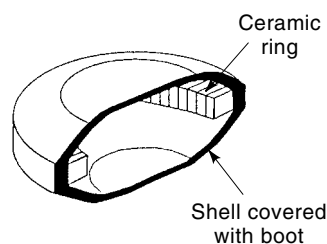


Figure 12. A ring shell projector. The mostly empty interior may contain a pressure relief system.

faces are dome-shaped shells affixed to the rim of a segmented ceramic ring. The open space between the domes contains an air bladder pressurized by sea water fed through a hydraulic low-pass filter to provide a compliant but statically balanced interior.

Flooded Ring. If the active element in Fig. 6 were removed from its housing, waterproofed, and placed in an acoustic free field, one would not expect it to make a very effective sound source because radiation from the inner surface of the ring would mostly cancel that from the outer surface. For particular frequencies, ring diameters, and ring heights, however, it can be a fairly efficient radiator. The radiation impedance for a ring radiating from all surfaces is difficult to predict, so most often the designs are based on McMahon's empirical findings (17). The overwhelming advantage of this design is that it should work at any ocean depth. The radiation pattern is omnidirectional in the plane containing the ring and has some directionality (which is beneficial in many applications) in the plane of its axis. Placing a flooded ring next to a hard baffle or coaxially with other flooded rings produces other useful radiation patterns.

Slotted Cylinder. A rectangular bilaminar plate wrapped into a cylinder with the ceramic on the inside is called a slotted-cylinder projector (Fig. 13). Originally developed to fit down oil drilling holes, this type has recently gained popularity for certain sonar applications. The advantages are small size for its frequency and good power-handling ability. The disadvantages are small relative bandwidth (a result of the small radiating area) and difficulty sealing the slot (where relative motion between opposite sides of the shell is high).

Hydroacoustic. Occupying a different camp than all of the other transducers reviewed, this high-power projector uses a piezoelectrically driven spool valve to modulate a high-pressure flow of hydraulic fluid which then vibrates opposing circular radiating faces (18) (Fig. 14). The input power to the actuator valve is small, and all of the acoustic power is extracted from the dc hydraulic pump. Therefore no electronic power amplifier is required, which reduces system cost somewhat. These sources are designed specifically for high output in the low and very low frequency ranges (10 Hz to 300 Hz) and are bulky and rugged. They are often rigged for towing from research vessels. Their main disadvantages are higher distortion than more conventional types and a reputation for poor reliability.

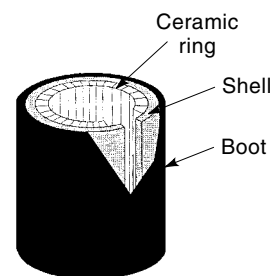


Figure 13. A slotted cylinder projector. The central post and end caps, similar to Fig. 6, have been omitted for clarity.

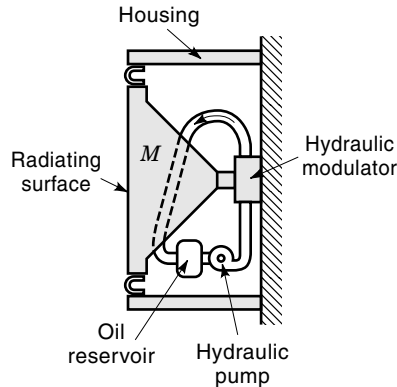


Figure 14. A vastly simplified cross section of one half of a hydroacoustic projector. The hydraulic modulator may be a piezoelectrically-driven spool valve.

Moving Coil. By adapting the drive mechanism used in a standard loudspeaker (Fig. 2) to underwater use one obtains a very low resonance frequency and, because it is usually operated above resonance, flat response over a very wide band. This transduction technique was one of the first to be developed, and it is still in use and being steadily improved (19) because of the advantages cited. Because of the electrodynamic driver, it has low electrical impedance. The main disadvantages are low efficiency, low source level capability, and sensitivity to operating depth.

Performance Requirements

Specifications of greatest interest to users and designers of underwater sound projectors are

- **Frequency range.** This may be specified as center frequency and Q (reciprocal of the fractional bandwidth) or as upper and lower band edge frequencies (usually at the -3 dB points of the transmitting response curve). Measurement factors affecting this quantity are which drive parameter (input voltage, current, or power) is to be held constant during the frequency sweep and where the monitoring hydrophone is placed.
- **Depth range.** Usually minimum and maximum depths for full power use and a maximum nonoperating (survival) depth are specified.
- **Impedance range.** Maximum power transfer from an electrical source depends on matching the source to the load impedance. Underwater transducers, especially highly efficient ones, show wide swings in both magnitude and phase of their electrical impedance with frequency, and this generally affects amplifier operation and achievable bandwidth. If long cables are involved, cable effects must also be considered.
- **Output source level.** This is normally specified as acoustic sound pressure level (SPL) in a certain direction over a given frequency band, scaled as if measured at a range of 1 m from the acoustic center of the source. The designer must be alert to several ancillary properties affected by drive level: voltage and current limits in the driver, cables, and connectors; mechanical stress levels within the transducer; thermal effects (see later); and potential for acoustic cavitation.

- **Directivity patterns.** Specified at several frequencies and in different planes through the acoustic center of the source.
- **Weight in air and in water.**
- **Ambient temperature range and duty cycle.** These are related because the internal heating rate depends on the duty cycle and power level, and the cooling rate is related to internal and ambient temperatures.

EVALUATION METHODS AND METRICS

Methods of Analysis

Three basic approaches are used to analyze a transducer. The first is directly solving the equations of motion for the electromechanical system. This proceeds like a forced vibration problem with electrically connected forcing functions either in the boundary conditions (for surface-force transduction) or in the stress/strain relations for the active material (for body-force transduction). Acoustic effects are accounted for by specifying a radiation impedance at the radiating surface. The second method is finite-element analysis (FEA) using an FEA code which handles coupled elastic/acoustic problems and offers electrically or magnetically active elements. The third is by translating the electroacoustic system into an equivalent electrical circuit by using an electromechanical analogy, then analyzing the equivalent circuit. Like the first, this method also requires knowledge of the radiation impedance.

Finite-element methods are gaining in popularity as specialized FEA programs become more widespread. These codes are expensive to acquire and use, however, and many runs are required to understand how critical performance parameters respond to variations in various dimensional and material choices. Reference 20 is a recent compilation of FEA programs suited for electroacoustic analysis. If the problem is amenable to equivalent circuit analysis, this method has the advantages of simplicity and provides immediate insight into design parameter sensitivities. The following simplified equivalent circuit analysis demonstrates the usefulness of the technique and illustrates several important transducer design principles.

Electromechanical Analogies and the Two-Port Network

Two analogies are commonly used in associating mechanical variables with conventional electric circuit quantities (see Table 1). The impedance analogy that connects current, the

Table 1. Electromechanically Analogous Quantities and Their Symbols

Mechanical Quantity	Electrical Quantity (Impedance Analogy)	Electrical Quantity (Mobility Analogy)
Force F	Voltage E	Current I
Velocity U	Current I	Voltage E
Displacement $x = \int U dt$	Charge $q = \int I dt$	
Impulse $\int F dt$		Charge q
Mass M	Inductance L	Capacitance C
Compliance C_m	Capacitance C	Inductance L
Mechanical Resistance R_m	Resistance R	Conductance G

“through” quantity, with velocity is best suited to electric field transducers and will be used following. The mobility analogy regards current as analogous to mechanical force, and it is more convenient for magnetic field transducers. In both cases the mechanical quantities are associated with *ideal* mechanical components: lossless, massless springs connected to perfectly rigid point masses and ideal massless dashpots.

Consider the transducer as a linear two-port network, as in Fig. 15, and assume a lumped-parameter system in which the essential mechanical behavior is described by a single vibrating mass. The projector is driven by voltage E and current I applied at the electric port. The resulting mechanical output appears at the opposite port where one can measure a force F and velocity U . There are six ways to formulate a pair of linear equations relating the four port variables E , I , F , and U . For electric field transducers it is convenient to choose E and U as the independent variables, and the equations are

$$\begin{aligned} I &= Y_b E - \phi U \\ F &= \phi E + Z_m^E U \end{aligned}$$

The names and SI units of the coefficients are as follows: $Y_b \equiv (I/E)_{U=0}$ is the blocked electrical admittance (in siemens, the reciprocal of ohm), $Z_m^E \equiv (F/U)_{E=0}$ is the short-circuit mechanical impedance (in newtons per meter per second or kilograms per second), and $\phi \equiv -(I/U)_{E=0} = (F/E)_{U=0}$ is the electromechanical transformation ratio (in newtons per volt or amps per meter per second).

Physical analysis of simple linear electric field transducers shows that the circuit parameters always have the following properties: $Y_b = G_b + j\omega C_b$, a capacitive susceptance shunted by a (usually small) conductance, ϕ is real and independent of frequency, and

$$Z_m^E = R_m + j\omega M + 1/j\omega C_m^E$$

where R_m is the internal mechanical resistance, M is the moving mass of the transducer, and C_m^E is the compliance (displacement over force) seen at the mechanical port when the electrical terminals are short-circuited.

Transition to a Single-Port Electrical Circuit

The mechanical port is terminated in a short circuit when the transducer is operated in a vacuum (nearly the same as in air) and in its radiation impedance when in water. The radiation termination is depicted as a series $R - L$ circuit having impedance $Z_r = R_r + j\omega M_r$, where the mechanical power dissipated in the real part R_r represents acoustic power radiated into the far field, and the kinetic energy stored in the radiation mass M_r represents acoustic energy stored in the near field. In general, Z_r varies with frequency. Combining all of the above relationships, the electrical behavior of the simple

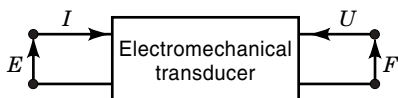


Figure 15. A linear two-port network having electrical variables (voltage and current) at the left hand port and mechanical variables (force and velocity) at the right hand port.

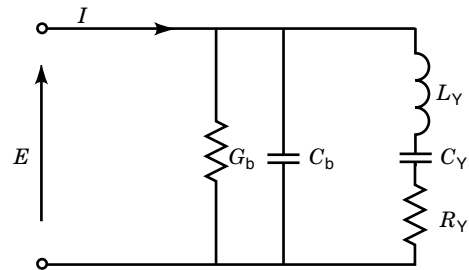


Figure 16. Simplified equivalent circuit of a lumped parameter, single degree-of-freedom, piezoelectric drive transducer. Subscript b denotes the blocked electrical components; Y the transformed mechanical components.

single degree-of-freedom projector, in water, is the same as that of the circuit of Fig. 16.

Capacitance C_b is called the blocked capacitance, which is shunted by a frequency-dependent conductance G_b to represent dielectric losses. These two elements form the entire circuit when the transducer is clamped (blocked) so that $U = 0$. The remaining three elements form the motional branch of the circuit and are transformed mechanical quantities given by

$$\begin{aligned} L_Y &= (M + M_r)/\phi^2 \\ C_Y &= \phi^2 C_m^E \\ R_Y &= (R_m + R_r)/\phi^2 \end{aligned}$$

Note that these transformations yield the proper electrical units. For instance, the units of $\phi^2 C_m^E$ are $(N/V)^2(m/N) = N \cdot m/V^2 = J/V^2 = \text{farad}$. The current flowing in the motional branch equals ϕU .

Relationship Between Circuit Element Values and Transducer Parameters

This single degree-of-freedom circuit has a single resonance and a number of auxiliary parameters which define the transducer near that resonance. Setting Z_r to zero supplies the in-air quantities. Resonance frequencies in air and in water are given by

$$\begin{aligned} \omega_{ra}^E &= (2\pi f_{ra}^E) = \frac{1}{\sqrt{L_Y C_Y}} = \frac{1}{\sqrt{M C_m^E}} \\ \omega_{rw}^E &= (2\pi f_{rw}^E) = \frac{1}{\sqrt{(M + M_r) C_m^E}} \end{aligned}$$

The mechanical storage factor Q_m has meaning only at resonance (the second subscript indicates which one). It describes the bandwidth over which the projector transfers power to the load and is defined as the ratio of energy stored in the inductive reactance per cycle to that dissipated in the resistance. High Q_m indicates a sharp resonant peak, and low values are usually desired, but this must be accomplished by making R_r rather than R_m large so as not to degrade the efficiency:

$$Q_{mw}^E = \frac{\omega_{rw}^E L_Y}{R_Y} = \frac{\omega_{rw}^E (M + M_r)}{R_m + R_r}$$

The electromechanical coupling factor k is a pivotal parameter related to bandwidth and power handling. For the case under study k^2 is defined as the ratio of the energy available in the motional branch to the total energy contained in that branch and the coupling element (the blocked capacitance in the case of ceramic transducers), ignoring losses.

$$k^2 = \frac{C_Y}{C_Y + C_b} = \frac{\phi^2 C_m^E}{\phi^2 C_m^E + C_b}$$

The dielectric dissipation factor $\tan\delta$ is the ratio of conductance to susceptance B_b for the blocked ceramic, the same as for ordinary capacitors. $\tan\delta$ is observed to be independent of frequency, so G_b must vary linearly with frequency.

$$\tan\delta = \frac{G_b}{B_b} = \frac{G_b}{\omega C_b}$$

The electric storage factor Q_e is the ratio of input susceptance to conductance at resonance. It is related to input power factor and, therefore, to the bandwidth over which the transducer accepts power from the amplifier. To achieve wide system bandwidth, Q_e for the water-loaded transducer should also be low. Denoting the electrical input admittance by $G_i + jB_i$,

$$Q_e = \frac{B_i(\omega_r)}{G_i(\omega_r)} = \frac{1}{\tan\delta + \frac{k^2}{1-k^2} Q_m}$$

Note that because a good quality transducer has both a low dielectric loss factor and a high Q_m in air, $\tan\delta \ll Q_m k^2 / (1 - k^2)$, which leads to a formula for calculating the coupling factor from in-air admittance data:

$$\frac{k^2}{1-k^2} = \frac{1}{Q_e Q_m}$$

Because either Q when high restricts the bandwidth, a sensible goal is to have their product as small as possible, and this implies maximizing k .

Overall projector efficiency is composed of two factors: η_{ma} which varies slowly with frequency and accounts for losses in the motional branch and η_{em} which is strongly frequency-dependent and accounts for losses on the electrical side. The η_{em} equation following is evaluated at mechanical resonance where it is a maximum, therefore the following expression for η_{ea} is also valid only at resonance:

$$\text{Mechanoacoustic efficiency: } \eta_{ma} = \frac{R_r}{R_m + R_r} \text{ (at any frequency)}$$

Electromechanical efficiency:

$$\eta_{em} = \frac{1/R_Y}{G_b + 1/R_Y} = \frac{1}{1 + \frac{\tan\delta}{\frac{k^2}{1-k^2} Q_m}} \text{ (at resonance)}$$

$$\text{Electroacoustic efficiency: } \eta_{ea} = \eta_{ma} \eta_{em} \text{ (at resonance)}$$

Measurement of Equivalent Circuit and Transducer Evaluation Parameters

Most transducer parameters are obtained solely from measurements at the electric terminals, with the source first in

air and then in water. The basic measurement is either impedance Z (measured at constant current) or admittance Y (at constant voltage). Generally ceramic-based drivers are best evaluated from admittance data, and magnetic drivers from impedance data. In certain situations plotting the magnitude of Z or Y versus frequency is sufficient. If practical, choose a drive level in air that excites mechanical amplitudes similar to those expected in water at the rated source level. (A limiting factor, however, may be tolerability of in-air sound levels in the vicinity of the measurement.)

The remainder of this section outlines some simple rules for extracting transducer parameters from Y and Z data. More detailed instructions are in Sections 2.7–2.9 of Ref. 6 and in (21). These procedures are sufficient to find all parameters of the one-port electric circuit of Fig. 16, but electric measurements alone cannot determine the electromechanical ratio ϕ for which it is necessary to make both a mechanical and an electric measurement.

Complex Z and Y data can be presented in two ways: parametrically, with the real part on one axis versus the imaginary part on the other and with frequency as the parameter; or as two separate curves plotted against frequency. The first method provides more diagnostic information to the practiced eye and can be the basis of all electric measurements if the frequency points are plentiful near resonance. For reasonable parameter values the electrical admittance of the simple transducer of Fig. 16 produces a slightly distorted circle (a loop) in the Y -plane, and measuring certain geometrical properties of this loop is the basis of transducer admittance analysis.

The blocked capacitance C_b cannot be measured directly—practical clamps are not stiff enough to immobilize a typical underwater projector. Instead one measures both the free capacitance, $C^F = C_b + C_Y$, at some frequency far below resonance, and the coupling factor (at resonance), then calculates $C_b = (1 - k^2)C^F$. This procedure is invalid if C_Y varies with frequency (i.e., not a single-degree-of-freedom lumped parameter system).

Q_m is obtained by finding three frequencies: the frequency of maximum G_i (resonance), and the two frequencies on either side of resonance where G_i drops to half its maximum value. Calling these, in increasing order, f_1 , f_r , and f_2 , $Q_m = f_r / (f_2 - f_1)$, that is, Q_m is the unitless ratio of the peak frequency to the spread between those frequencies where the input power is half what it is at resonance.

The two resonant efficiency factors can be estimated from air and water admittance loop diameters D_{Ya} and D_{Yw} . These expressions for efficiency are valid only at isolated resonances of lumped-parameter transducers. The final determination of efficiency always requires both acoustical and electrical measurements:

$$\eta_{ma} = 1 - \frac{D_{Yw}}{D_{Ya}}$$

$$\eta_{em} = \frac{D_{Yw}}{G_i(\omega_r)}$$

Acoustical Power Derived from the Simple Equivalent Circuit

Two useful quantities related to the projector in Fig. 16 are the voltage-limited acoustic output power and the associated

input volt-amperes, both at resonance:

$$P_{AC} = \eta_{ma} \omega_{rw} Q_{mw} C_b E^2 \frac{k^2}{1 - k^2}$$

$$|E||I| = \frac{P_{AC}}{\eta_{ma}} \sqrt{1 + Q_e^2}$$

where E and I are the rms drive voltage and current at the input terminals. A few observations are in order:

- although low Q_m is desirable for wide bandwidth, the resonant output boost of a high Q device relates directly to increased source level per volt;
- the factors C_b and E^2 separately depend on electrode spacing, but their product depends only on electric field strength, ceramic dielectric constant, and volume of active material;
- high coupling factor greatly benefits electrically limited output power;
- $\sqrt{1 + Q_e^2}$ is the reciprocal of the power factor of the transducer, as seen by the amplifier.

Centrality of Coupling Factor

The transducer coupling factor k plays a crucial role in many aspects of projector performance. The previous equations show how it influences both electrically limited output power levels and bandwidth. More fundamentally, it is an index of physical realizability for all transducers ($0 \leq k < 1$). This inequality is a consequence of static stability criteria for surface-force types and of the thermodynamics of the active material for body-force types. The coupling factor is an easily measured single quantity which indicates overall transducer quality and shows the relative impact of design or construction modifications. Furthermore, it serves as a means of comparing different transducer types.

The connection between k and bandwidth originated with Mason (22) who stated that an optimally loaded and electrically tuned projector has an attainable fractional bandwidth given by $k/\sqrt{1 - k^2}$. Stansfield (8) explored this topic in greater detail and found that the upper limit on system bandwidth depends on the properties of the power amplifier and the transducer. Assuming optimum tuning and an amplifier which tolerates a 2:1 variation in the magnitude of load impedance and a $\pm 37^\circ$ variation in phase angle (requirements corresponding to a power factor of better than 0.8), then the

optimum kQ_m product is ~ 1.2 , and the corresponding system bandwidth limit equals $0.8k/\sqrt{1 - k^2}$. Note that achieving a certain Q_m does not by itself produce the desired bandwidth. The coupling must also be close to its optimum value of $1.2/Q_m$.

In view of these facts, projector designers are advised to pay attention to design choices which affect k . The first rule for increasing k is to minimize the impact of electrical or mechanical elements that store energy but do not participate in the coupling process. For example, a small electric field transducer on a long cable suffers reduced coupling because the cable capacitance stores uncoupled electric energy. Coupling reduction also arises from added compliance, such as stress rods, waterproofing seals, and pressure relief systems. The reduction occurs whether the parasitic element is added mechanically in series or in parallel with the main vibrating member and even if it resonates at the transducer resonance. For distributed-parameter body-force transducers, k can be improved by design adjustments that produce greater strain uniformity in the active material. This is why ceramic can be removed from the central, low stress region of a bender plate without incurring a coupling penalty.

Electrical Tuning

Most water-loaded projectors display poor power factors (large electric phase angle) near resonance. This may be improved by inserting a tuning network between the amplifier and the transducer. Magnetic-drive transducers have a net inductive impedance at resonance and so are tuned with added capacitance, whereas electric-field transducers are the reverse and are tuned with inductors. Tuning does not degrade coupling if the external tuning elements add reactance of the opposite sign to that used in the electromechanical coupling process.

Hybrid magnetostrictive/piezoelectric transducers (23) combine both types of driver materials and have the interesting property of being self-tuning.

NEW HIGH-POWER DRIVER MATERIALS

Three challenges continue to motivate underwater projector technology: obtaining smaller size-to-wavelength ratios, higher output power, and wider bandwidth. During the past forty years a series of low-frequency transducer innovations (bender bar, flextensional, Terfenol-driven flextensional, bar-

Table 2. Properties of Active Materials^a

	Unbiased PZT-8	Biased PZT-8	Terfenol-D	PMN-PT (1% La)	PZN-PT (no prestress)
ρ (kg/m ³)	7600	7600	9100	7800	8300
s_{33}^E (pm ² /N)	17	16	34.5	13	150
$\epsilon_{33}^T/\epsilon_0$	1500	1900		13000	2800
d_{33} (pm/V)	300	280		515	1800
k_{33}	0.69	0.59	0.67	0.42	0.93
max \mathcal{E}_3 (rms MV/m)	0.39	0.85		0.62	0.7
$k_{33}^2 \epsilon_{33}^T \mathcal{E}_3^2$ (kJ/m ³)	0.81	3.6	4.9	8.0	10.5

^a All except PZN-PT prestressed to 40 MPa.

rel-stave flextensional, slotted-cylinder) have steadily, but incrementally, advanced our capabilities. Recently the focus has shifted toward finding improvements in active materials to make bigger strides in performance.

The development of Terfenol-D was the first step in this direction. Its low sound speed and high energy density permit smaller or lower frequency sources without compromising output power level. Recently new classes of electrostrictive ceramics have emerged. Many of these materials are based on lead magnesium niobate (PMN) mixed with various additives, notably titanates of lead, strontium, and barium. Another nascent material is single-crystal, lead zinc niobate mixed with small amounts of lead titanate (PZN-PT). Some of these new materials exhibit astoundingly high dielectric constants and electrically induced elastic strains, but these benefits are paid for by other less desirable qualities, such as frequency dispersion, strong temperature dependence, and a quadratic strain/field relationship. If the desirable large-signal properties can coexist with low $\tan\delta$ and good mechanical strength and if they can be preserved during the transition from laboratory specimens to production lots, these materials could propel new advances in the state of the art for high-power, low-frequency projectors.

These emergent materials may be compared with conventional ones through the concept of field-limited energy density. All projectors have some limit on output power level. Depending on frequency and operating environment, the limit may be mechanical (stress, displacement, or cavitation limits), electrical (voltage or current limits), or thermal (runaway heating). It is usually desirable to arrange things so that the electric limit controls in the usual operating domain, and in this case one can compare material power handling capacities based on the electromechanical energy density, $k_{33}^2 \epsilon_{33}^T \mathcal{E}_3^2$. In this expression k_{33} is the material coupling coefficient (similar to the transducer coupling factor k applied to the material itself), ϵ_{33}^T is its dielectric permittivity at zero stress, and \mathcal{E}_3 is the maximum allowed rms electric field strength.

Table 2 lists pertinent properties for four active materials: a standard high-power piezoelectric ceramic (PZT-8), the modern magnetostrictive material Terfenol-D, one variety of PMN-PT, and single-crystal PZN-PT. The analogous magnetic field-limited energy density, $k_{33}^2 \mu_{33}^T H^2$, is given for Terfenol-D. All data are for the material under a reasonable compressive prestress, except for PZN-PT where such data did not exist when the data survey was made (24,25). Because the new high-strain materials require a dc bias to achieve quasi-linear operation, PZT-8 is evaluated both in its normal, prepolarized (unbiased) state and with an external dc bias like the other entrants. In every case the bias field (not stated) is chosen to optimize the material's high ac-field properties. Loss parameters are not included in the table.

The materials in Table 2 are arranged in order of increasing energy density in the last row. The first observation is that operating PZT-8 with a dc bias results in slightly reduced coupling k_{33} and piezoelectric strain coefficient d_{33} but a significant increase in energy density because of the higher allowed driving field. Terfenol-D has coupling comparable to unbiased PZT-8, but much higher energy density and about twice the compliance modulus which, together with its higher mass density, leads to a much lower sound speed and a corresponding size advantage. Although it has a lower coupling than PZT, PMN-PT offers similar elastic properties and much

larger dielectric constants resulting in a greatly increased energy density. These properties, combined with its low hysteresis and very high strain capabilities, make PMN an attractive new material for future projector designs. Though unproved in actual use, PZN offers the promise of even greater energy density and very impressive coupling. However its extremely high compliance may have implications for the mechanical design.

BIBLIOGRAPHY

1. J. E. Blue and A. L. Van Buren, Transducers, in M. J. Crocker (ed.), *Encyclopedia of Acoustics*, Vol. 1, New York: Wiley, 1997, pp. 600–604.
2. R. S. Woollett, Basic problems caused by depth and size constraints in low-frequency underwater transducers, *J. Acoust. Soc. Amer.*, **68**: 1031–1037, 1980.
3. F. V. Hunt, *Electroacoustics*, Cambridge, MA: Harvard Univ. Press, 1954.
4. E. L. Hixson and I. J. Busch-Vishniac, Transducer principles, in M. J. Crocker (ed.), *Encyclopedia of Acoustics*, Vol. 4, New York: Wiley, 1997, Chap. 159.
5. R. S. Woollett, *Sonar Transducer Fundamentals, Section I: General Transducer Theory*, Newport, RI: Naval Underwater Syst. Center, 1988.
6. O. B. Wilson, *Introduction to Theory and Design of Sonar Transducers*, 2nd ed., Los Altos, CA: Peninsula, 1988, Sect. 5.2.
7. R. S. Gordon, L. Parad, and J. L. Butler, Equivalent circuit of a ceramic ring transducer operated in the dipole mode, *J. Acoust. Soc. Amer.*, **58**: 1311–1314, 1975.
8. D. Stansfield, *Underwater Electroacoustic Transducers*, Bath, UK: Bath Univ. Press, 1991.
9. R. S. Woollett, *Sonar Transducer Fundamentals, Section II: The Longitudinal Vibrator*, Newport, RI: Naval Underwater Syst. Center, 1988.
10. R. S. Woollett, Theory of the piezoelectric flexural disk transducer with applications to underwater sound, U.S. Navy Underwater Sound Laboratory, USL Res. Rep. No. 490, 1960.
11. R. S. Woollett, *The Flexural Bar Transducer*, Newport, RI: Naval Underwater Syst. Center, 1986.
12. M. D. McCollum, B. F. Hamonic, and O. B. Wilson (eds.), *Transducers for Sonics and Ultrasonics*, Lancaster, PA: Technomic, 1993.
13. K. D. Rolt, History of the flextensional electroacoustic transducer, *J. Acoust. Soc. Amer.*, **87**: 1340–1349, 1990.
14. G. A. Brigham, Analysis of Class-IV flextensional transducer by use of wave mechanics, *J. Acoust. Soc. Amer.*, **56**: 31–39, 1974.
15. G. W. McMahon and B. A. Armstrong, A pressure-compensated ring-shell projector, *Conf. Proc., Transducers Sonar Appl.*, Birmingham, UK: Inst. of Acoustics, 1980.
16. B. A. Armstrong and G. W. McMahon, Discussion of the finite element modeling and performance of ring shell projectors, *IEE Proc.*, (Part F) **131**: 275–279, 1984.
17. G. W. McMahon, Performance of open ferroelectric ceramic cylinders in underwater sound transducers, *J. Acoust. Soc. Amer.*, **36**: 528–533, 1964.
18. J. V. Bouyoucos, Hydroacoustic transduction, *J. Acoust. Soc. Amer.*, **57**: 1341–1351, 1975.
19. B. S. Willard, A towable, moving-coil acoustic target for low frequency array calibration, U.S. Naval Underwater Syst. Center, NUSC Tech. Rep. No. 6369, 1981.
20. C. Scandrett, ed., *Proc. Transducer Modeling Workshop*, Monterey, CA: Naval Postgraduate School, 1997.

21. G. E. Martin, Determination of equivalent circuit constants of piezoelectric resonators of moderately low Q by absolute-admittance measurements, *J. Acoust. Soc. Amer.*, **26**: 413–420, 1954.
22. W. P. Mason, *Electromechanical Transducers and Wave Filters*, 2nd ed., New York: Van Nostrand, 1948.
23. J. L. Butler, S. C. Butler, and A. E. Clark, Unidirectional magnetostrictive/piezoelectric hybrid transducer, *J. Acoust. Soc. Amer.*, **88**: 7–11, 1990.
24. M. B. Moffett et al., Biased lead zirconate-titanate as a high-power transducer material, U.S. Naval Undersea Warfare Center Division, NUWC-NPT Reprint Rep. 10766, 1997.
25. M. B. Moffett and J. M. Powers, Single crystal PZN/PT as a high-power transduction material, U.S. Naval Undersea Warfare Center Division, NUWC-NPT Tech. Memo. 972127, 1997.

WILLIAM J. MARSHALL
BBN Technologies